THE USE OF PLASTIC MEDIA IN A MOVABLE BED MODEL TO STUDY SEDIMENTARY PROCESSES IN RIVERS

By

Jean-Rene Thelusmond

B.S., State University of Haiti, School of Agronomy and Veterinary Medicine, 2006

A Thesis

Submitted in partial fulfillment of the requirements for the degree of
Master of Science

Department of Civil and Environmental Engineering
Graduate School
Southern Illinois University Carbondale
December 2011

UMI Number: 1506853

Dissertation Publishing

UMI 1506853

THESIS APPROVAL

THE USE OF PLASTIC MEDIA IN A MOVABLE BED MODEL TO
STUDY SEDIMENTARY PROCESSES IN RIVERS

By

Jean-Rene Thelusmond

A Thesis Submitted in Partial

Fulfillment of the Requirements for the Degree of

Master of Science

in the field of Civil and Environmental Engineering

Approved by:

Dr. Lizette R. Chevalier, Chair

Dr. Bruce A. Devantier

Dr. Matt Whiles

Graduate School
Southern Illinois University Carbondale
August 16, 2011

AN ABSTRACT OF THE THESIS OF

JEAN-RENE THELUSMOND, for the Masters of Science degree in CIVIL ENGINEERING,

presented on August 16, 2011, at Southern Illinois University Carbondale.

TITLE: THE USE OF PLASTIC MEDIA IN A MOVABLE BED MODEL TO STUDY

SEDIMENTARY PROCESSES IN RIVERS.

MAJOR PROFESSOR: Dr. Lizette R. Chevalier

The use of plastic media was evaluated for modeling sedimentary processes in rivers

using a moveable bed model (MBM). From gradations within the range of 0.17-2 mm, the size

of the thermoset plastic media was color coded in order to better visualize complex flow

processes. Equations developed by Engelund-Hansen (1967) and Schoklitsch (1962) were used

to predict sediment transport in order to establish the type of bed channel typified by the

media. Similitude and scaling principles were used in order to create a virtual river reach as a

replica of the model. Based on the physical properties of the media and data collected during

simulations, the results suggest that the thermoset plastic media can be used to model coarse sand

and gravel in MBM.

DEDICATION

This work is dedicated to my beloved wife Lita and our soon-to-be-born son Wisdel together with my affectionate mother Marie and my dear uncle Aleus-Paul.

ACKNOWLEDGEMENTS

TABLE OF CONTENTS

LIST OF TABLES

LIST OF FIGURES

LIST OF NOTATIONS

A	Channel's flow resistance coefficient
A_a	Area
A_{ar}	Area scale ratio
$BDLT$	Bed load transport
C_f	Total resistance coefficient
C_c	Coefficient of curvature
C_u	Uniformity coefficient
D	Particles diameter
D_m	Model's particles diameter
D_p	Prototype particles diameter
D_{50}	Particles median diameter
f	Mass of sediment per unit with of channel
Fr_m	Model's Froude number
Fr_p	Prototype's Froude number
Fr_r	Froude number scale ratio
g	Gravitational accelaration
g_b	Specific mass transport
i_b	Specific submerged mass transport
k	Roughness height
L_r	Length scale ratio
MBM	Movable bed model

ρ	Density of water
ρ_s	sediment density
Q	Flow rate
q	Specific discharge
q_o	Critical value of q for initial of motion
q_t	Dimensionless total bed material transport per unit width
q_t*	Dimensionless total bed material transport per unit width
$Re*$	Particle Reynolds number
$Re*_m$	Model's particle Reynolds number
$Re*_p$	Prototype particle Reynolds number
S_o	Channel's slope
τ	Bed shear stress
$\tau*$	Dimensionless Shield number
$\tau*_m$	Model's dimensionless Shield number
$\tau*_p$	Prototype dimensionless Shield number
σ	Surface tension
γ	Specific weight of water
γ'	Submerged particle specific weight
t	Time of travel
t_r	Hydraulic time scale
$(T_s)_r$	Sediment timescale
U	Velocity of water
u_*	Critical shear velocity

υ	Kinematic viscosity
X_m	Model's length
X_p	prototype's length
X_r	Horizontal scale
Y_m	Model's depth
Y_p	prototype's depth
Y_r	Vertical scale

CHAPTER 1

INTRODUCTION

Engineers and other scientists have studied sedimentation in waterways throughout

history. Some civilizations had formerly used trial and error to study and solve sediment

transport problems pertaining to irrigation channels (van Rijn 1993). Researchers have become

interested in sedimentation because of the heavy burdens it imposes to the physical and the biotic

environment. Sedimentation reduces soil fertility, decreases surface drainage in floodplains,

damages valuable crops, and intensifies the frequency and risks of flooding. Accumulation of

sediment in some engineering infrastructures may disrupt the infrastructures, impose additional

maintenance costs, reduce functionality and decrease service life. Therefore understanding

mechanism of sedimentation and designing effective approach for mitigating its adverse impact

has been a challenge for researchers and professionals.

Sedimentation is a complex phenomenon that involves both the flow of the water as well

as the physical characteristics of the channel. Researchers have applied various techniques

including field studies, movable bed modeling, and numerical modeling to advance our

understanding of this complex phenomenon. Though field studies can provide data of good

quality, they might be time consuming and expensive, depending on their magnitude. In addition,

the interplay of too many variables in the natural environment makes the interpretation of the

field data difficult (Dalrymple 1985). Numerical models are less time consuming and less

expensive than field studies and movable bed models. However, there are some complicated flow

and sediment transport situations (e.g. local scour of alluvial bed sediment around pier,

submerged pipelines, design of water in-take for hydropower stations etc.) for which hydraulic modeling, including movable bed models, is more reliable than analytical solution or computer simulation (Ettema et al. 2000).

As noted by Ettema et al. (2000), movable bed models are generally used to simulate and elucidate processes such as flow over loose planar bed, flow with bed forms, sediment transport rates, and local patterns of flow and sediment movement around hydraulic structures. In such cases, the issues of scaling and similitude must be addressed with respect to the soil and the fluid. Since it is unlikely to achieve hydraulic and morphological similarity simultaneously, Sharp (1981) recognized that the morphological processes that result from the hydrodynamic forces applied to the movable bed model are of primary importance, whereas the hydrodynamic effects are of secondary importance when applying scaling and similitude principles. In early research on the issue of scaling and similitude, Warnock (1950) suggested that complete similitude was not achievable, recommending that modeling focus on using a combination of several incomplete similitudes. Hughes (1993) reported that geometrically scaling down non-cohesive sediment resulted in cohesive soil, in essence creating soil dynamically different from the prototype. He suggested using sediment with different densities as well as scaling size.

A variety of bed materials such as sand, crushed coal, pumice, burnt shale, bakelite, sawdust, ground walnut shells, and different types of plastics have been used to replicate river bed sediment (Foster 1975). Sand and crushed coal have been used by the US Army Waterways Experiment Station (WES) to simulate the beds of different rivers (Sharp 1981; Franco 1978; Foster 1975) whereas ground walnut shells have been used to replicate the Missouri River sand with respect to gradation, settling, bar and dune formation (Sharp 1981). Sand provides the advantage of being inexpensive and readily available. However, its use is impractical for the

study of sediment movement in small models where the velocity of water is too low to move the sediment. In addition, ripples tend to form in the river bed due to the small grain size of the sand typically used (Sharp 1981). In addition, wet sand is heavy and hard to handle. Crushed coal has been used because of its low density (5.5 times lighter than sand) (Franco 1978). But, crushed coal ripples when large quantity of small grain size is used at a water temperature less than 60°F. This is generally only a concern for outdoor models. Alternatively, plastic media is available in a variety of sizes, shapes, colors, and specific gravity. However, when their specific gravity is less than 1.3, the surface tension of the water causes the media to float (Franco 1978). For example, an experiment conducted with acrylic as bed sediment was abandoned in the middle of the process because of floatation of the bed material (Gaines 2002).

To address the issue of floating sediment, a higher density thermoset plastic media, color-coded by size, has been used as bed-material (Gough 2011). The thermoset plastic (e.g. melamine) is produced from recycled stock of plastic trays and dinnerware. Hence, it is extensively available and affordable (< US$ 4.5/kg). By grinding different color stock to different sizes, Gough has demonstrated a visually effective means to study sediment transport in river bed models that cannot be replicated with sand or coal.

The overall scope of this research was to further test the use of the thermoset plastic media to model sediment transport. Using a movable bed model (MBM) developed by Little River Research and Design (Carbondale, IL), experiments were conducted to further test the properties of the thermoset plastic media and to evaluate the extent of its use in small scale models.

CHAPTER 2

BACKGROUND

2.1 Physical Model

Various types of models are used in research, including models of hydraulic structures

(Ettema et al. 2000), and simplified process models (Parker1998). Models of hydraulic structures

investigate hydro-mechanical phenomenon important to civil and mechanical engineering, and

geomorphology (Ashmore 1991; Warburton and Davies 1994). These hydraulic models have

typically been classified into two categories, fixed bed models with non-erodible boundaries &

no sediment transport and movable bed models (MBMs) with freely movable substrate (Peakall

et al. 1996; Raghunath 1967).

Movable bed models are miniature streams that replicate the characteristics of related

watercourses, providing some adjustments are made. The principles of similarity constitute the

basis of the procedures involved in physical modeling. Given MBMs entail the existence of two-

phase flow (water and sediment), it follows that both water movement and sediment movement

need to be modeled (Sharp, 1981). However, being a complex task, modelers often resort to

approximations while modeling two-phase flow (Yalin 1971).

2.2 Similitude

Similitude implies complete accord of various processes between a model and its

prototype. Models can be similar to their prototypes in three different ways, namely, geometric

similarity, kinematic similarity, and dynamic similarity. Geometric similarity implies that the

shape of the model is the same as that of the prototype, whereas kinematic similarity signifies

equality of ratios of velocity and acceleration. On the other hand, dynamic similarity means that

the corresponding forces have similar ratio in the model and the prototype. In movable bed river models, strict geometric similarity is not always pursued for economic and practical reasons. A model that is geometrically similar or undistorted may require a lot of space for its accommodation, particularly if it is large. In terms of practicality, an undistorted model may not develop sufficient tractive force to transport the bed material. The foregoing compels modelers to choose different scale ratios for horizontal and vertical dimensions. When this occurs, the resulted model is known as a distorted model.

There is still debate as to whether or not distortion should be applied in modeling. However, some researchers consider it as undesirable, yet inevitable. In spite of providing some advantages, some investigators suggest that it should be avoided in MBMs as much as possible (Jaeggi 1986; Glazik 1984). Although Glazik (1984) suggests avoiding distortion in MBMs, he noted that a distortion ratio (ratio of horizontal scale to vertical scale) of 1.5 is acceptable. In contrast, Ettema et al. (2000) suggests that distortion should be limited to 6 in MBMs whereas Sharp (1981) suggests a limit between 6 and 7.

As noted by Ettema et al. (2000), flow of water and sediment in channels with non-cohesive particles can be represented by this functional relationship:

$$A = f_A(\rho, v, \sigma, k, Y, S_o, U, g) \tag{2.1}$$

In case of uniform and steady flow, the above relationship is modified for a movable bed model as follows:

$$A = f_A(\rho, v, D, \rho_s, Y, S_o, U, g) \tag{2.2}$$

or as:

$$A = f_A(\rho, v, D, \rho_s, Y, u_*, \gamma') \tag{2.3}$$

where:

A= channel's flow-resistance coefficient,

f = mass rate of sediment per unit width of channel,

ρ = density of water,

v= kinematic viscosity of water,

σ= surface tension,

k= roughness height,

Y= depth of flow,

S_o= channel slope,

U= velocity of water,

g= gravitational acceleration,

ρ_s= sediment density,

D= particle diameter,

$\gamma' = (\rho_s - \rho)g$= submerged specific weight of sediment particles,

$u_* = (gYS_o)^{1/2}$= critical shear velocity.

By applying Buckingham-Pi theory (Ettema et al. 2000), the equation (2.3) can be rewritten in dimensionless form as equation (2.4). Since the equation contains seven independent variables (n=7) and three fundamental dimensions, four dimensionless parameters can be generated from it.

$$\Pi_A = f_A \left[\frac{u_* D}{v}, \frac{\rho u_*^2}{\gamma' D}, \frac{Y}{D}, \frac{\rho_s}{\rho} \right] \tag{2.4}$$

According to Maynord (2006), the dependent variables A and Π_A might represent flow resistance, thalweg sinuosity, sediment transport, or some other variable in fluvial channel. The parameters presented in equation (2.4) are necessary to establish similitude (Waldron 2008). The first term on the right hand side (u_*D/v), called Particle Reynolds Number (Re^*), is the ratio of the viscous forces and inertial forces acting on each grain of sediment. The second term ($\rho u_*^2/\gamma'D$), known as Shields Parameter (τ^*) or Shield Number (also Shield Dimensionless Shear Stress or Particle Mobility Number) is extremely important in sediment transport (Maynord 2006; Ho et al. 2010). The Shield Parameter is the ratio of bed shear stress i.e. $\tau = \rho u_*^2$ to the submerged weight of the particle. Shield parameter plays an important role in defining the amount of movement of the particle on the bed (Maynord 2006). The third term (Y/D) is the ratio of the depth to the particle grain size; it defines the surface tension effects, and it is often neglected in MBMs. The buoyant force on the sediment represented by the density of the sediment over the density of water (ρ_s/ρ) is also generally ignored because the second term has already contained it.

2.3 Scaling

Sharp (1981) considers the geometric scale, which depends on the fluid and model size, as the fundamental scale for hydraulic model. He defines it as the ratio of some length in the model to its counterpart in the prototype. Mathematically, $X_r = X_m/X_p$, where X_r is the model-to-prototype ratio of a variable X; and the subscripts "m" & "p" represent model & prototype, respectively. These notations will be adopted throughout the next sections.

According to Ettema et al. (2000), when flows are driven by gravity (e.g. open channels) the main dynamic similarity criteria that needs to be satisfied is the Froude number, and the

Froudian similarity is met when the ratio of forces represented by $Fr_r = U_r/(g_r L_r)^{1/2} = 1$ as illustrated in equation (2.5).

$$Fr_r = \frac{Fr_m}{Fr_p} = \frac{U_m (gY_m)^{-1/2}}{U_p (gY_p)^{-1/2}} = 1 \qquad (2.5)$$

The above equation can be rewritten as: $\dfrac{U_m}{U_p} \dfrac{(Y_p)^{1/2}}{(Y_m)^{1/2}} = 1$

Therefore noting that $Y_r = Y_m/Y_p$, velocity can be derived from: $U_r = \dfrac{U_m}{U_p} = (Y_p)^{1/2}(Y_m)^{-1/2}$ as:

$$U_r = (Y_r)^{\frac{1}{2}} \qquad (2.6)$$

Based on equation (2.6), the flow rate can be obtained by establishing a relationship between area (A_a) and velocity (U). Let Q designate the flow rate, then $Q = UA_a$, where $A_a = YX$. Therefore,

$$Q_r = U_r.A_{ar} = (Y_r)^{\frac{1}{2}}.Y_r.X_r \text{ which yields,}$$

$$Q_r = (Y_r)^{\frac{3}{2}}.X_r \qquad (2.7)$$

Since time of travel is the ratio of length to velocity ($t = X/U$), the dynamic timescale is determined as follows:

$$t_r = \frac{X_r}{(Y_r)^{\frac{1}{2}}} \qquad (2.8)$$

2.4 Sediment modeling

Sediment is scaled so that it can move in a corresponding manner both in the prototype and in the model. In lightweight models (LWM), similarity between model and prototype implies that Shield Parameter (τ^*) also called densimetric Froude number must be the same in the prototype and the model (Hughes 1993). In addition, the grain size Reynolds number (Re^*) should be equal in the model and the prototype. Sharp (1981) presented the following equations for scale ratios:

$$\tau_r^* = \left(\frac{u_*^2}{(\gamma'/\gamma)D} \right)_r = 1 \tag{2.9}$$

$$(Re^*)_r = \left(\frac{u_* D}{\nu} \right)_r = 1 \tag{2.10}$$

A relationship is derived for the sediment size and density using equations (2.9) and (2.10) as follows:

$$\frac{\gamma_m'}{\gamma_p'} = \left(\frac{u_{*m}}{u_{*p}} \right)^2 \frac{D_p}{D_m} \tag{2.11}$$

and

$$\frac{D_m}{D_p} = \frac{u_{*p}}{u_{*m}} \tag{2.12}$$

Equations (2.11) and (2.12) give a relationship between particle size and specific weight:

$$\frac{\gamma_m'}{\gamma_p'} = \left(\frac{D_p}{D_m} \right)^3 \tag{2.13}$$

Sedimentation timescale is different from Froude number or hydraulic timescale for some processes (e.g. dunes and bars) (Ettema et al. 2000). As defined by Ettema et al. (2000), bed-load time scale is the time for a transport rate Q_s to fill a volume X^2Y of bed space. However, sedimentation timescale is not straightforward. Zwamborn (1966) established an approximate relationship between hydraulic timescale and sediment timescale $(T_s)_r$ after he verified a number of models against their prototypes. This relationship is expressed as:

$$(T_s)_r \approx 10 t_r \tag{2.14}$$

2.5 General guidelines for the selection of model sediments

Due to the impracticality of scaling the bed material of the prototype to the scale of the model, it is important to select a model bed material that will behave in a similar fashion as that of the prototype (Foster 1975). As stipulated by Raghunath (1967), the major factors that determine the suitability of a bed material are fundamentally the cost and the availability of the material, in addition to its constant specific gravity. Furthermore, a long exposure of the material to water should give rise neither to swelling nor to formation of lumps (Raghunath 1967). Some general guidelines for the selection of a model bed material as suggested by the Ettema et al. (2000) include the following:

i. The model sediment must be denser than the model fluid;

ii. Individual sediment particles or low concentrations of particles should not float as result of surface tension forces;

iii. The particles should not break down or suffer alterations in size or shape due to abrasion or decay when transported;

iv.   The model water visibility should not be reduced because of the discoloration of the media;

v.   The sediment diameter should not be less than 0.7 mm lest the bed of the model forms ripples.

The thermoset plastic media was tested against these guidelines stated above in order to find out if it satisfies the necessary criteria to be used in modeling. Because of limited time and resource constraints, the third criterion was left for future research.

2.6 Thermoset plastic sediment material

Thermoset plastics are plastic materials synthesized from condensation polymerization reactions. Their chemical structure is composed of crossed-linked chains. Melamine formaldehyde and urea formaldehyde are two amino-plastics that form these types of materials. Melamine formaldehyde is known to be hard, resistant to heat and staining (Whelan 1994), and it tends to resist any alteration of its physical integrity. Therefore, ground melamine formaldehyde media obtained from Composition Materials Company was used as sediment material in this experiment.

2.7 Gravel bed channels and sand bed channels

Gravel bed channels and sand bed channels can be distinguished by their bed material size and their slope (Thorne et al. 1997). For gravel bed channels, the grain size varies from 2mm to 60mm (Rocha 1990), and the slope varies from 0.05 to 0.5 (Thorne et al. 1997). In contrast, the grain size of sand bed channels is less than 2mm whereas their slope is ≤0.1 (Thorne et al. 1997). This means that the bed forms characteristics along with velocity profiles, flow resistance and sediment transport will be different in each type of channel (Thorne et al.1997). In this

thesis, a sand bed equation and a gravel bed equation will be used to compute bed-load transport in the Emriver model. The end results will help us determine whether the thermoset plastic media used in the model can be typified as a sand bed river or a gravel bed river, or both.

2.8 Prediction equations

Engelund-Hansen [(1967)]* equation for sand bed and Schoklitsch [(1962)]* equation for gravel bed are the two sediment transport relations used in the present study. Engelund-Hansen relation as mentioned by Garcia (2008) takes the form

$$C_f q_t^* = 0.05(\tau^*)^{5/2} \tag{2.15}$$

C_f= total resistance coefficient (skin friction plus form drag) expressed as:

$$C_f = \frac{gYS_o}{U^2} \tag{2.16}$$

τ^*= total (skin friction plus form drag) Shield stress based on the size D_{50}, expressed as:

$$\tau^* = \frac{YS_o}{(\rho_s - \rho)D_{50}} \tag{2.17}$$

q_t^*= dimensionless form for dimensionless total load material transport per unit width, expressed as:

$$q_t^* = \frac{q_t}{\sqrt{\gamma' D_{50}} D_{50}} \tag{2.18}$$

The original work of the authors was not consulted.

q_t= total volume transport rate of bed load material per unit width (m^2/s),

 Y= depth of flow (m),

U= flow velocity (m/s),

S_o= channel slope.

According to Young (1989), the Schoklitsch equation is expressed as follows:

$$g_b = 2.5 \rho S_o^{3/2} (q - q_o) \qquad (2.19)$$

where:

g_b= specific mass transport rate (kgm^{-1}s^{-1}),

ρ= density of water,

q= specific discharge (m^2/s),

q_o= critical value of q for initiation of motion (m^2/s).

$$q_o = \frac{0.26}{S_o^{7/6}} (\rho_s / \rho - 1)^{5/3} (D_{40})^{3/2} \qquad (2.20)$$

Another expression for the above equation for specific submerged mass transport is:

$$i_b = \frac{2.5 \rho S_o^{3/2}}{\rho_s / \rho - 1} (q - q_o) \qquad (2.21)$$

where ρ_s is the density of the sediment, and the other symbols represent the variables as defined

before.

CHAPTER 3

MATERIALS, EQUIPMENT AND METHODS

3.1 The movable bed model

The movable bed model used in this research was constructed by Little River Research &

Design. The Emriver model or Em4 was built on a 4mx1.5m platform (Figure 3.1) that facilitates

the adjustment of its slope. The model was designed so that it could be tilted in three axes (i.e. x,

y, and z). Having an octagonal shape, the Em4 is equipped with two reservoirs located in the

upstream and downstream. The reservoirs are connected to each other by tubing so that water can

recirculate. Flow was introduced at the head of the model through a 45-cm diameter cylinder

called energy dissipater unit (EDU). The apparatus of the upstream reservoir includes two pumps

and a magmeter. One of the pumps supplies the model with water whereas the other removes

water from the system. The magmeter continually displays the digital volumetric flow rate. The

downstream reservoir is a collection box that receives water and sediment from the model

through an adjustable standpipe. It has a pump filter that separates sediment from water. This

assures that only the sediment free water is returned to the upstream reservoir. A hose connected

to a tap replenishes both reservoirs with water. The Em4 is also equipped with two cranks

located in the downstream end. One of these cranks allows the model to be tilted (right and left)

whereas the other allows the model to be inclined forward or backward (Figure 3.1).

Figure 3.1: Photograph of the Em4

3.2 The sediment bed material

The bed material employed as sediment in the model was a mixture of ground plastics color coded by size: red, brown, white, and yellow. As specified by the manufacturer, the material size for each color was 0.4 mm, 0.7mm, 1 mm, and 1.4 mm, respectively (Figure 2.1). Sieve analysis was performed (with US standard sieves) in order to determine the size distribution of the particles. Random sampling technique was used in order to sample the bed of the model. A total of 12 samples of approximately 100 grams each were collected and sieved. The results of the sieve analysis showed no difference between the samples in terms of size distribution; therefore, the size distribution of only one sample was retained for the present study. The uniformity coefficient (C_u) and the coefficient of curvature (C_c) were computed using equations (3.1) and (3.2).

$$C_u = \frac{D_{60}}{D_{10}} \qquad (3.1)$$

$$C_c = \frac{(D_{30})^2}{D_{10}D_{60}} \qquad (3.2)$$

where D_{10}, D_{30} and D_{60} represent = 10%, 30%, and 60% finer by weight.

Figure 3.2: Photograph of the Coded by Size Thermoset Plastic Media

A specific gravity test was also performed for the thermoset plastic media. Three samples of media weighing 100 grams each were taken from each color. The weight (W_1) of a clean and dry volumetric flask filled with de-aired, distilled water up to 500ml was taken. The temperature of the water ($T=T_1{}^o C$) was 19°C. Each sample of the thermoset plastic media (100 g), previously dried in an evaporating dish, was then transferred to the volumetric flask. Water was added into the flask containing the media and air was removed from the mixture by a vacuum pump or aspirator. De-aired, distilled water (500 mL) was added to the flask. Next, the combined mass of

the flask, the sediment, and the water (W_2) was determined before pouring the media and water

into an evaporating dish. The media was dried in an oven set at 130°C for 8 hours, and its mass

(W_s) was measured. The equations below (Das 2002) were used to calculate the specific gravity

of the media.

$$G_{s(at-T_1^\circ C)} = \frac{W_s}{W_w} \tag{3.3}$$

where: $W_w(g) = (W_1 + W_s) - W_2$, mass of equal volume of water as

sediment. Based on specific gravity at a given temperature, the specific

gravity based on the value of the density of water at 20°C (G_s) was also

calculated (Equation 3.4).

$$G_{s(at20^\circ C)} = G_{s(at-T_1^\circ C)} \left[\frac{\rho_{(at-T_1^\circ C)}}{\rho_{(at T_{20}^\circ C)}} \right] = G_{s(at-T_1^\circ C)} G \tag{3.4}$$

Where: $G = \dfrac{\rho_{(at-T_1^\circ C)}}{\rho_{(at T_{20}^\circ C)}}$, and ρ= density of water.

3.3 Experimental procedure

The model was filled with the thermoset plastic media to a depth of about 7-9 cm before

each run began. The bed of the Em4 was molded, and a straight channel having a V shape along

with a flood plain was created. The slope of the channel was set by adjusting the standpipe. Then,

the flow was set at 90 mL/s in order to saturate the bed of the model with water. Once the bed

was saturated, the flow was adjusted to the desired value for the run and kept constant. The flow

rate was recorded at the beginning and at the end of each run. This was done by using an

FMG3001-PP flow meter manufactured by Omega Engineering, Inc. The flow meter was tested

for accuracy by using graduated cylinders/beakers and a stopwatch. The volume of water

collected over time was compared to the flow rate recorded by the flow meter. Different ranges

of flow were tested; the mean error between recorded and measured flow rate was estimated to be

5.3%.

A sediment feeder was used to feed sediment into the stream at a feeding rate of 2 g/s.

The sediment feed rate was constantly adjusted in order to get equilibrium which was determined

by observation and measurement. Equilibrium was assumed to take place if the following

conditions were satisfied: incoming sediment rate equal to outgoing sediment rate and absence of

incision or deposition in the downstream of the channel. The velocity of water was measured in a

1-2 m stream by injecting dye as the equilibrium of the channel was closely verified. The leading

edge of the dye was followed over the preset distance by using a stopwatch. Three measurements

were made, and the average velocity   was taken as the final velocity.

Cross sections of the model were also measured repeatedly with a cross-beam and a

leveling rod along with a laser in order to record water surface elevation. First, a datum of 300

mm was determined with the laser. Distance to water surface (DWS) was measured at several

points along a horizontal line (HL) in the model (Figure 3.3). In each measurement point, the

vertical distance to the streambed and the corresponding horizontal distance (HD) were recorded

(Figure 3.2). Water elevation (calculated by subtracting the VD from the datum) was plotted

versus the horizontal distance (Figure 3.4). The data generated was used to calculate flow width

and flow depth (FD) necessary to predict bed load transport (BDLT) in the model. Flow depth

was computed by the difference between the water surface and the water elevation. Similarly,

flow width was calculated by the difference between the *x*-coordinates of the tangential points (Figure 3.3). Three transects were measured for each run. Bed load transport was captured from the standpipe using a funnel and cone filter (mesh size: 190 μm) for about 6 to10 seconds every five minutes. The number of samples captured for each run varied between 5 and 10. The captured media was dried in an oven at 180 °F for two hours. Then the average weight was recorded. Eight experimental runs were performed with various combinations of flows and slopes. The experimental data is presented in Table 3.1. Engelund-Hansen's and Schoklitsch's equations were used to calculate sediment transport rate. The Froude number was also calculated for each run.
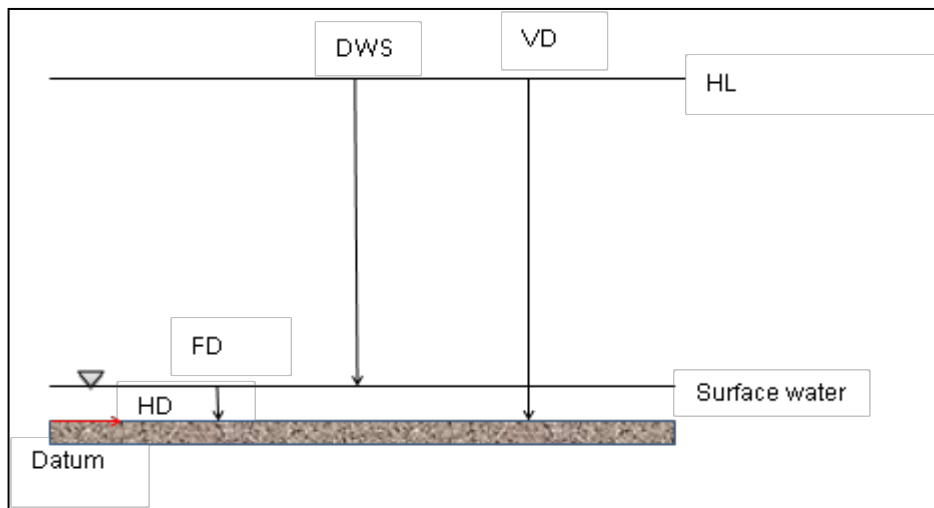
Figure 3.3: Model's Cross-sections Measurement
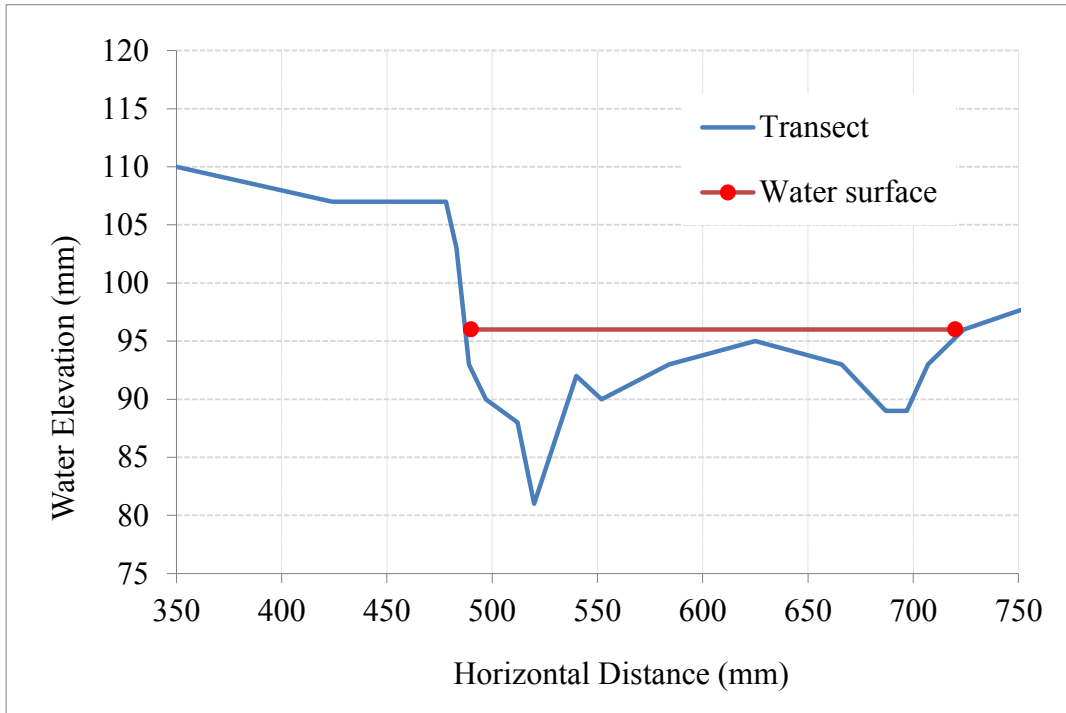
Figure 3.4: Transect for Flow Depth and Channel Width Measurement

Table 3.1: Run Conditions and Bed Load Transport Rate

Run No	Slope	BDLT Rate (g/s)	Flow Rate (mL/s)	Velocity (m/s)	Flow Depth (m)	Channel Width (m)
1	0.03	2.87	100	0.168	0.002	0.45
2	0.03	2.76	100	0.188	0.00184	0.439
3	0.03	6	157	0.260	0.00285	0.326
4	0.03	5	157	0.240	0.003	0.389
5	0.02	1.89	100	0.130	0.002	0.425
6	0.02	2.2	100	0.120	0.0023	0.400
7	0.02	4.5	157	0.150	0.0035	0.367
8	0.02	4	157	0.140	0.0037	0.451

3.4 Modeling principles

The principles of similitude and scaling were applied in order to create a virtual river reach by using the characteristics of the model under study. The following parameters were determined from the model in order to infer the corresponding parameters for the prototype: length (X_m) = 4m; depth (Y_m) = 0.002 m; Slope (S_m) =0.04; maximum flowrate (Q_m) = 4.7×10^{-4} m³/s; Velocity (U_m) = 0.17m/s; D_{50}= 0.94 mm. Then, geometric scales and Froudian scales were determined. Furthermore, the conditions under which the motion of the particles in the virtual prototype would be similar to the model were investigated

Before choosing the horizontal and vertical scales, it was assumed that the model was distorted (i.e. the horizontal scale would be different from the vertical scale). Under this assumption, the choice of a wide range of horizontal and vertical scales was made based upon previous models. Raghunath (1967) and Allen (1952) reported a range of scales that have been recommended in model studies. For a distorted river model, the horizontal scales range from 1:100-1:1000 whereas the vertical scales range from 1:20-1:100. Based on the recommendations reported by Raghunath (1967) and Allen (1952) along with other researchers (e.g. Sharp 19981; Ettema et al. 2000; Gaines 2002), a range of horizontal scales (1:100-1:900) and vertical scales (1:20-1:600) were chosen. The scaled length of the river reach for different scales was calculated using the equation below:

$$X_p = \frac{X_m}{X_r} \qquad (3.5)$$

where X_p, the length of the prototype, X_m, the length of the model, and X_r the ratio of the model to the prototype. Based on the vertical scale and the depth of the model, the depth of the prototype for different scales was also calculated by using the following equation:

$$Y_p = \frac{Y_m^{1/2}}{Y_r^{1/2}} \tag{3.6}$$

Y_p= prototype's depth

Y_m= model's depth

Y_r= vertical scale

The depth of the model was varied on purpose in order to find the corresponding depth and velocity in the prototype. A distortion factor of 3.5 (i.e. half of the distortion recommended by Ettema et al. (2000) in physical modeling) was assumed; therefore, the horizontal and the vertical scales were selected among the range of scales tested. The measured depth of the water in the model was estimated to be 0.002 m; but 0.02m was assumed as depth for the model so that a river depth close to a real river could be calculated. Using the foregoing geometric scales, the Froudian scales were determined by the following equations:

$$U_r = (Y_r)^{1/2} \tag{3.7}$$

$$Q_r = A_{ar}U_r = (X_rY_r)(Y_r)^{1/2} = X_rY_r^{3/2} \tag{3.8}$$

$$t_r = \frac{L_r}{U_r} = \frac{X_r}{\sqrt{Y_r}} \tag{3.9}$$

Q_r= discharge ratio

t_r= hydraulic time scale ratio

L_r= length scale ratio

The bed slope of the prototype was also calculated by using the following relationship:

$$\frac{S_m}{S_p} = \frac{Y_m / X_m}{Y_p / X_p} \tag{3.10}$$

3.5 Sediment mobility

In order to evaluate the mobility of the thermoset plastic media, two dimensionless

parameters were used: Shields stress (τ^*) and particle Reynolds number (Re*) expressed as:

$$\tau^* = \frac{u^{*2}}{(\gamma'/\gamma)D} \tag{3.11}$$

and:

$$Re^* = \frac{u^*D}{\nu} \tag{3.12}$$

Where $u^* = \sqrt{gYS_o}$ and $\gamma' = (\gamma_s - \gamma)g$

u^*= critical shear velocity,

Y= depth of water,

S_o= slope,

ν = kinematic viscosity of water,

D= median size particle diameter,

γ'=submerged specific weight of sediment particle.

If $(\tau^*)_m = (\tau^*)_p$ and $(Re^*)_m = (Re^*)_p$, it would be concluded that sediment transport was similar in the model and the prototype. If not, it would be dissimilar, which would imply that initiation of sediment motion and bed load transport along with regime of sediment motion are not the same in the model and the prototype (Fan and Le Méhauté 1969).

3.5 Grain size scaling and sediment timescale

The thermoset plastic media was scaled up by using the equations below (Sharp 1981):

$$\frac{\gamma'_m}{\gamma'_p} = \frac{(u^*_m)^2}{(u_p^*)^2} \frac{D_p}{D_m} \tag{3.13}$$

and

$$\frac{D_m}{D_p} = \frac{u_p^*}{u_m^*} \tag{3.14}$$

The above equations yield the following relationship between particle size and specific weight (Sharp 1981):

$$\frac{\gamma'_m}{\gamma'_p} = \left(\frac{D_p}{D_m}\right)^3 \tag{3.15}$$

D_m = diameter of the model sediment

D_p = diameter of the prototype sediment

The sediment timescale was calculated by using the Zwamborn (1966) relation that approximates sediment timescale to ten times hydraulic timescale.

Therefore, $(T_s)_r = 10t_r$, where $(T_s)_r$ is sediment time scale and t_r is the hydraulic timescale.

CHAPTER 4

RESULTS AND DISCUSSION

This research compared the thermoset plastic media used as sediment in the Emriver

model to other model sediments. Size gradations and specific gravity of the media were tested.

The type of bed channel typified by the thermoset plastic media was also examined by using the

Engelund-Hansen (1967) sand bed equation and the Schoklitsch (1962) gravel bed equation. In

the end, scaling and similitude principles were applied to derive hydraulic and sedimentary

characteristics of a virtual river reach based on analogous characteristics of the model.

4.1 Properties of the thermoset plastic

The material size gradations (Figure 4.1) show that the thermoset plastic used in this

experiment has a median size of 0.94 mm. Sieve analysis of the media indicates the percentage

and the particles size of each color (Figure 4.2). The yellow particles constitute more than 30% of

the media and have particles size of 1.18 and 2 mm. The white particles with a diameter of 0.85

mm represent about 40% of the mixture. Meanwhile, the brown particles occupy about 14% of

the media and have a size of 0.425 mm. The red particles account only for 1.5% with particles

size between 0.17-0.25 mm. Thermoset plastic median diameter is in the range of the median

diameter of other lightweight sediments used in modeling (Table 4.1).

Table 4.1: Thermoset Plastic D_{50} versus Other Lightweight Sediments

Lightweight Sediment	Median size (D_{50}) (mm)	Source
Ground walnut shells	0.30	(Bettess 1990)
Bakelite	0.85	
Polystyrene	1-2	
Perspex	0.3-0.37	
Thermoset plastic	0.94	The present study

The uniform coefficient (C_u) and the coefficient of curvature (C_c) for the thermoset plastic media are presented in Figure 4.1. The media is classified as poorly graded soil since C_u= 2.5<6 and C_c=0.85<1 (Das 2002).

$C_{u=}2.5$
$C_c=0.83$
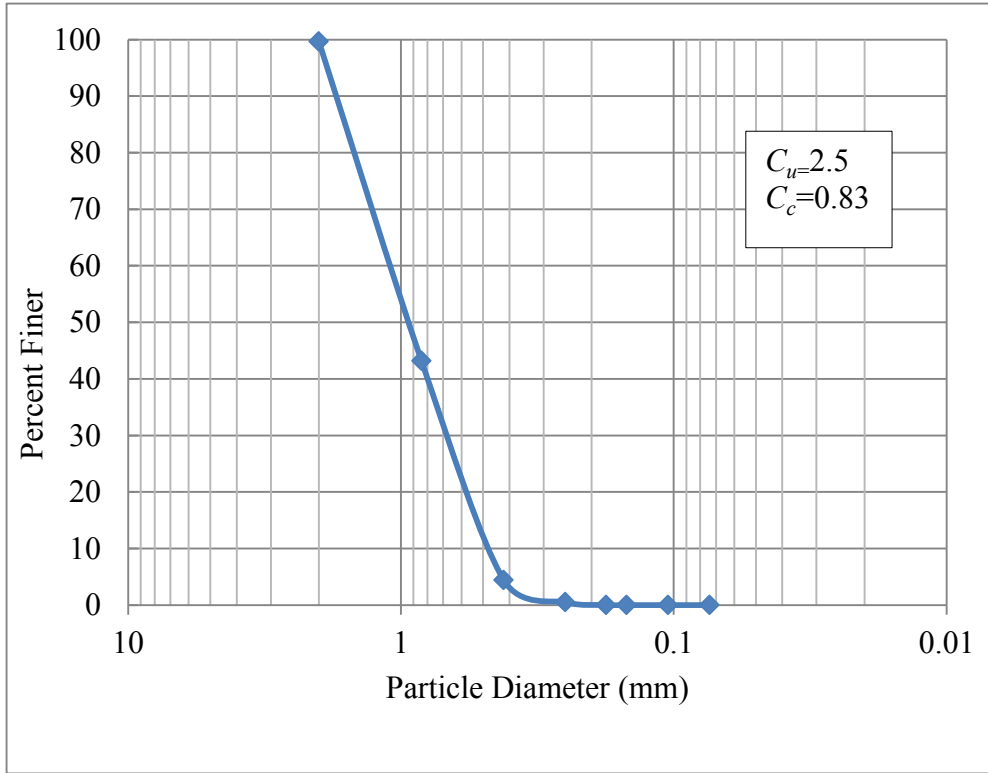
Figure 4.1: Thermoset Plastic Sediment Material Gradation Curve
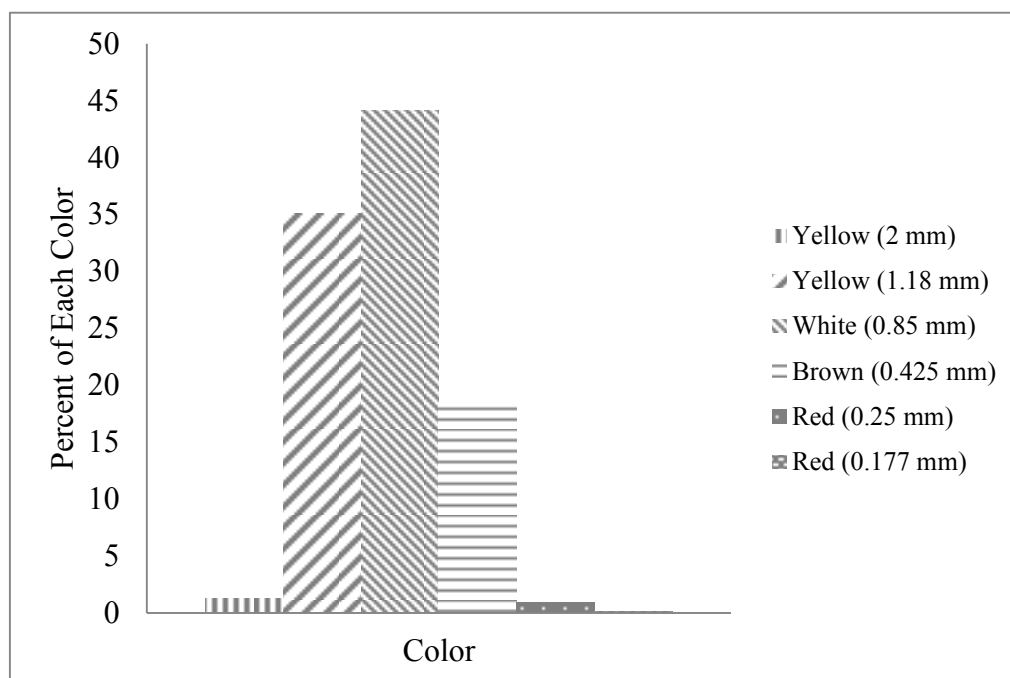
Figure 4.2: Thermoset Plastic Media: Size and Percentage of Each Color

The mean specific gravity for individual and combined colors is presented in Table 4.2

Table 4.2: Specific Gravity of Thermoset Plastic Material

Number of samples	Color	Average specific gravity
3	Red	1.53
3	Brown	1.54
3	White	1.47
3	Yellow	1.56
3	Combined colors	1.54

The average specific gravity was measured as 1.54± 0.07 for the combined colors. A comparison

of this specific gravity was made against other model sediments reported by Ettema et al. (2000).

Figure 4.3 shows that thermoset plastic is ranked third after sand and lucite. Equally important is

that the media falls in the optimal range of specific gravity (1.2-1.6) for model sediment (Figure 4.3).
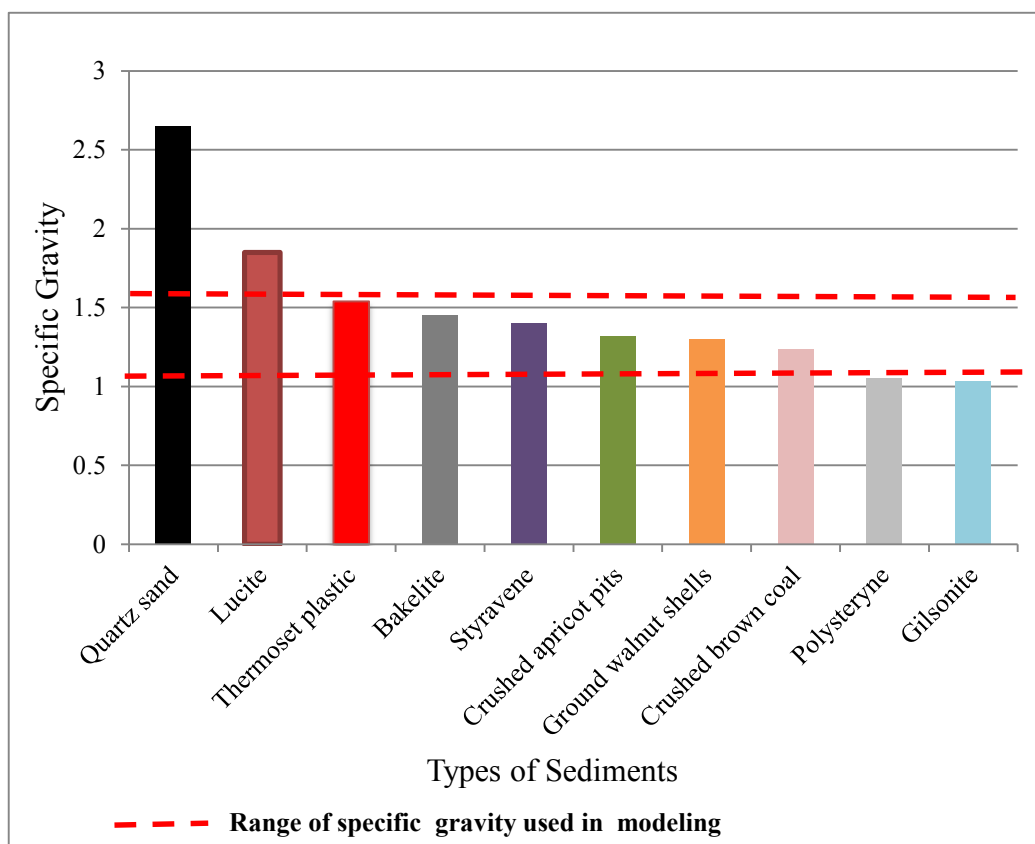
Figure 4.3: Typical Specific Gravity for Model Sediments

4.2 Prediction of sediment transport rate

Two sediment transport equations were used in the present study: the Engelund-Hansen (1967) equation (2.15), and the Schoklitsch (1962) equation (2.19). These equations were applied in order to determine if the thermoset plastic media used in the model could relate to a sand bed river or a gravel bed river, or both.

The Engelund-Hansen relation is applied only for sand bed river with relatively uniform bed sediment. Though developed from a small laboratory dataset, the Engelund-Hansen formula also performs well in the field (Garcia 2008).

Schoklitsch on the other hand, derived his formula from a previous equation that he generated in 1934 from experiments performed on sand bed physical models. He also used sand and gravel bed load data gathered from Gilbert's 1914 flume experiments. In 1962, Schoklitsch calibrated his formula by using both field and laboratory data. The Schoklitsch equation has been applied for engineering practices in rivers with coarse sediments (Young and Davies 1990). While Engelund-Hansen's relation was developed to compute bed material load or total load, Schoklitsch's relation was developed to compute bed load.

The sediment transport rate predicted by the Engelund-Hansen equation was compared to the measured sediment transport rate (Table 4.3). The Engelund-Hansen equation under-predicts sediment transport rate by 71.6% on average. The Froude number influenced the predictive capacity of the Engelund-Hansen equation. The Engelund-Hansen relation yields better performance in runs 1 and 2 where Froude numbers are 2.71 and 2.5, respectively. In contrast, in run 7 where the Froude number is the lowest, the Engelund-Hansen relation performs poorly. Therefore, the predictive capacity of the Engelund-Hansen relation depends partly on the values of the Froude number. Yang and Wan (1991) tested the accuracy of eight bed material load formulas, including the Engelund-Hansen formula. They found that the Engelund-Hansen relation was ranked second in terms of accuracy when tested for laboratory datasets. However, when tested for river datasets, the same formula was ranked seventh for accuracy. Therefore, as noted by Yang and Wan (1991), the accuracy of a given formula is tributary of the hydraulic and sedimentary conditions that prevail in a certain environment.

Likewise, comparisons between measured and predicted bed load transport (BDLT) rate are detailed in Table 4.4 for the Schoklitsch equation. The percent difference between measured and estimated bed load transport averages 70. Bed load transport rate is better predicted in runs 1

and 2 (Table 4.4). However, in runs 7 and 8, the percent difference between measured and predicted bed load transport is high (e.g. 88.6% and 90%, respectively). Bravo-Espinosa et al. (2003) evaluated the Schoklitsch relation and concluded that the Schoklitsch formula yields better performance in partially transport-limited and supply-limited conditions. In the present experiment, sediment availability was rather unlimited, for sediment was supplied not only through the erosion of the bank and the bed of the channel, but also through the sediment feeder.

Table 4.3: Engelund-Hansen (1967) Sediment Transport Predictions

Run No	Slope	Froude Number	Measured BDLT $(m^2/s)*10^6$	Predicted BDLT $(m^2/s)*10^6$	$\dfrac{\text{Measured}}{\text{Predicted}}$	Percent Difference
1	0.03	2.71	18.4	9.54	1.96	48
2	0.03	2.5	12.85	7.4	1.75	42.7
3	0.02	1.56	12.26	2.1	5.9	82
4	0.03	1.96	6.28	1.9	3.2	69
5	0.03	1.7	6.37	1.7	3.8	73
6	0.02	1.46	8.87	1.61	5.5	81
7	0.02	1.24	5.5	0.65	8.4	88
8	0.02	1.35	4.44	0.59	7.6	86

Average discrepancy ratio…….4.76
Average percent difference……………….71.6%

Table 4.4: Schoklitsch (1962) Sediment Transport Predictions

Run No	Slope	Froude Number	Measured BDLT $(m^2/s)*10^6)$	Predicted BDLT $(m^2/s)*10^6$	$\dfrac{Measured}{Predicted}$	Percent Difference
1	0.03	2.71	18.4	8.55	2.2	53.5
2	0.03	2.5	12.85	6.68	1.9	48
3	0.2	1.56	12.26	2.95	4.2	75.9
4	0.03	1.96	6.28	2.45	2.6	61
5	0.03	1.75	6.37	2.32	2.8	63.7
6	0.02	1.46	8.87	1.91	4.6	78.5
7	0.02	1.24	5.5	0.63	8.8	88.6
8	0.02	1.35	4.44	0.43	10.3	90

Average discrepancy ratio…….4.67
Average percent difference… …....................70%

Figures 4.4, 4.5, and 4.6 are plots of the predicted and measured values for sediment transport. The solid line represents the condition of perfect agreement, whereas the dash lines represent the discrepancy ratios (r), $BDLT_{measured}/BDLT_{predicted}$, of 0.5, 2, and 4. The plots of Engelund-Hansen's and Schoklitsch's equations are presented in Figures 4.4 and 4.5 for slopes 0.02 and 0.03, respectively. As it can be seen in Figure 4.4, none of the data points fall within the discrepancy ratios of 0.5≤r≤2 for both Engelund-Hansen's and Schoklitsch's equations when the slope is 0.02. However, 25% of the data obtained from the Schoklitsch formula has a discrepancy ratio between 2 and 4 for the slope 0.02. On the other hand, 50% of the data points fall within 0.5 ≤r≤2 for each equation when the slope is 0.03 (Figure 4.5). Similarly, 50% of the data that has a discrepancy ratio between 2 and 4 for each formula when the slope is 0.03 (Figure 4.5). It appears in Figure 4.5 that Engelund-Hansen's and Schoklitsch's equations yield better results with

greater slope. This finding is in agreement with the results found by Yang and Wan (1991) as they evaluated the accuracy of different bed material load formulas by employing various parameters (e.g. slope, Froude number, concentration) with fluctuating values. The accuracy of the formulas, including the Engelund-Hansen equation, varied depending on the measured values of the slope, Froude number, and concentration of the sediment.
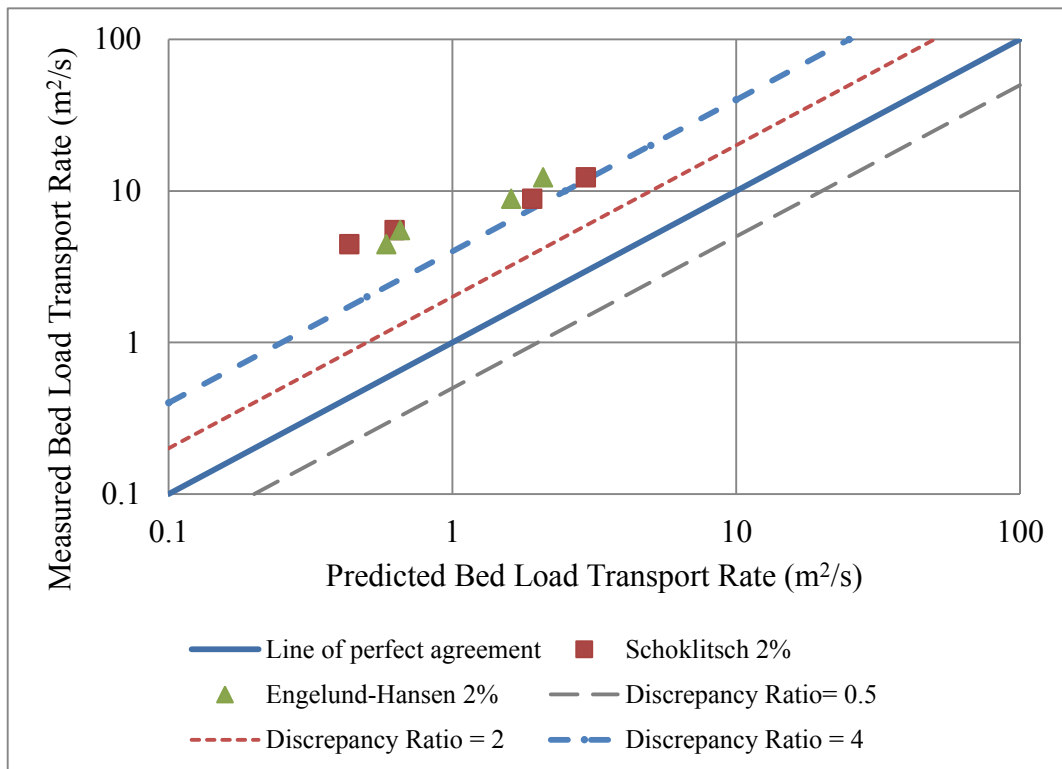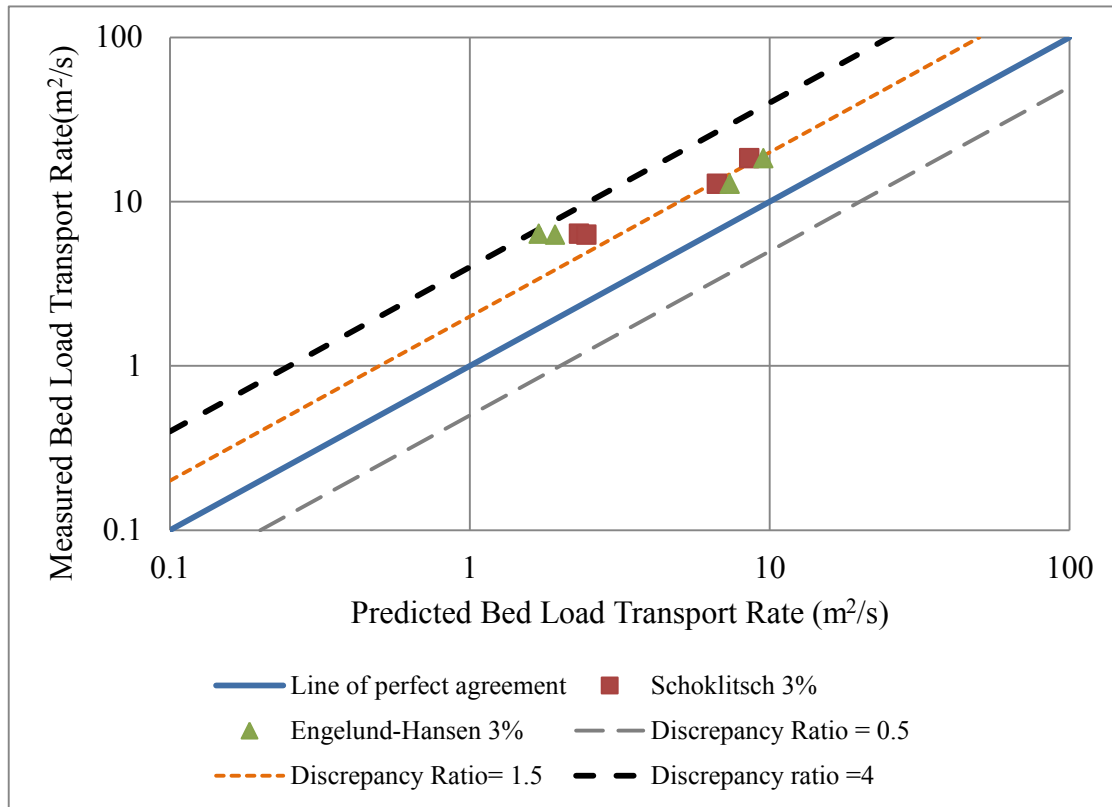

Figure 4.4: Sediment Transport Rate Predictions by the Engelund-Hansen (1967) and the Schoklitsch (1962) Equations for Slope 2%

Figure 4.5: Sediment Transport Rate Predictions by the Engelund-Hansen (1967) and the Schoklitsch (1962) Equations for Slope 3%

The summary of the sediment transport rate for the equations under consideration is presented in Figure 4.6. By inspection of the graph, it is apparent that 18.8% of the data points are within the discrepancy ratio range of 0.5 and 2, whereas 31.3% fall between 2 and 4. Therefore, Engelund-Hansen's and Schoklitsch's formulas made a fair prediction of sediment transport. As evidenced in Figure 4.6, all the data points are distributed in one side of the line of perfect agreement. In addition, all the data points for both equations are close to each other. If we stick to the predictions of Engelund-Hansen's and Schoklitsch's equations, we can consider the thermoset plastic media both as coarse sand and gravel. This finding is consistent with the configuration of the bed of the model subject to the flow (Figure 4.7).
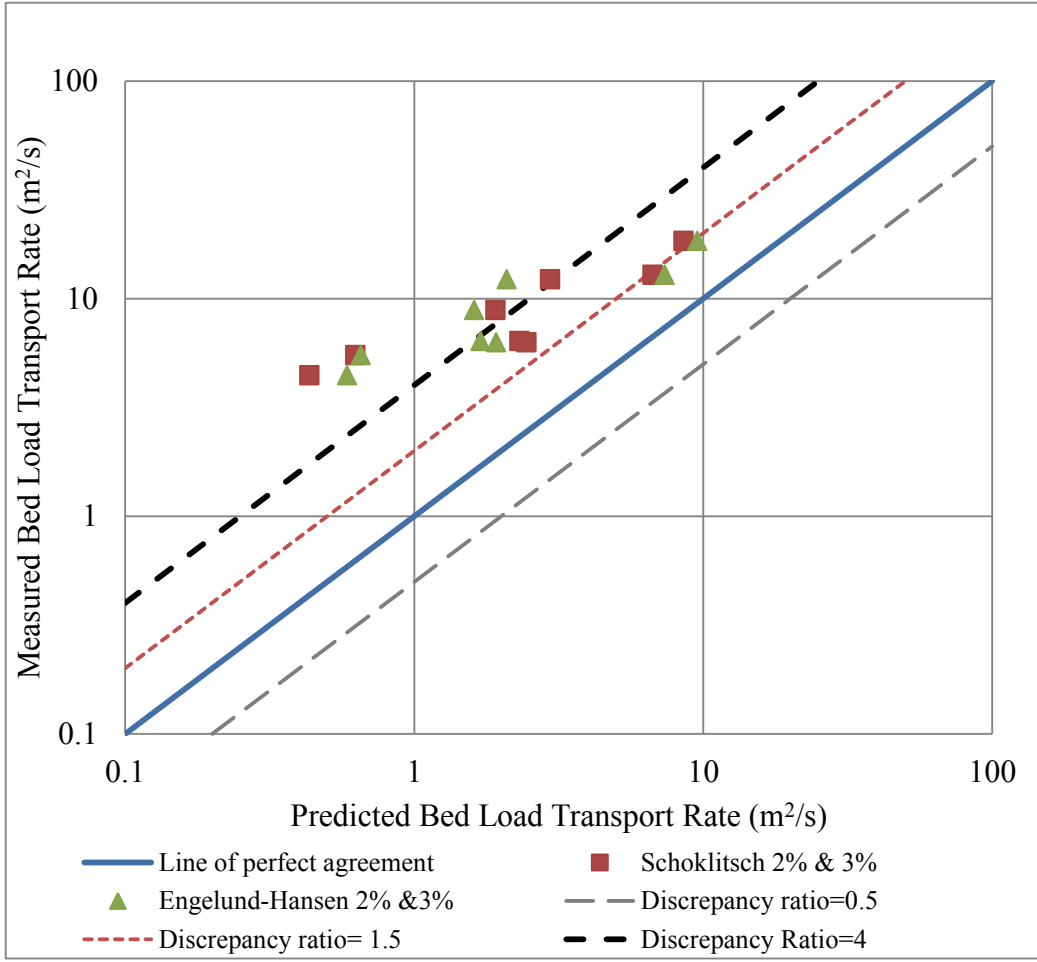
Figure 4.6: Summary of Sediment Transport Rate Predictions by the Engelund-Hansen (1967) and the Schoklitsch (1962) Equations for Slopes 2% and 3%

Figure 4.7: Bed of the Em4 after Two Hours of Flow

4.3 Similitude considerations

After reviewing the scaling and similitude laws, a virtual river reach was generated by using the hydraulic and sediment characteristics of the physical model under consideration. This approach was adopted here because there was no given prototype associated with the model. The reasoning that was made while choosing this approach "reverse modeling" was that if a model could be constructed by using the hydraulic and sediment characteristics of a prototype, it should also be possible to generate a prototype by using similar factors from the model. Using geometric scaling, hydraulic scaling, and sediment material scaling, the river reach described herein was created.

The maximum length of the Emriver model was estimated to be 4 m. The lengths of river the model can replicate range from 400 m to 4000 m depending on the values of the horizontal scales (Table 4.5). The stream length the model can simulate increases as the selected horizontal scales decrease.

Table 4.5: Horizontal and Vertical Scales & Respective Scaled Lengths and Depths

X_r	X_p (m)	Y_r	Y_p (m) for X_m=0.002 m	Y_p (m) for X_m=0.02 m	Distortion factor
1:100	400	1:20	0.04	0.63	5
1:150	600	1:30	0.06	0.77	5
1:200	800	1:40	0.08	0.89	5
1:250	1000	1:50	0.1	1	5
1:300	1200	1:60	0.12	1.09	5
1:350	1400	1:70	0.14	1.2	5
1:400	1600	1:80	0.16	1.26	5
1:450	1800	1:90	0.18	1.34	5
1:500	2000	1:100	0.2	1.41	5
1:550	2200	1:120	0.24	1.54	4.58
1:600	2400	1:140	0.28	1.67	4.28
1:650	2600	1:150	0.3	1.73	4.33
1:700	2800	1:200	0.4	2	3.5
1:750	3000	1:300	0.6	2.44	2.5
1:800	3200	1:350	0.7	2.64	2.28
1:850	3400	1:400	0.8	2.82	2.13
1:900	3600	1:600	1.2	3.46	1.5

The vertical scales selected range from 1:20 to 1:600 (Table 4.5). For a given vertical scale, the depth of the prototype increases as the depth of the model increases (Figure 4.8). Likewise, the velocity increases as the depth is increasing in the model or in the prototype (Figure 4.9). This fact is very important in the selection of the vertical scale. As evidenced in those results, the depth of the model will determine whether the model can be used to model a river that has a known depth. As noted by Sharp (1981), the depth of the model should be chosen in order to induce enough turbulence and roughness in the model and to facilitate measurement.
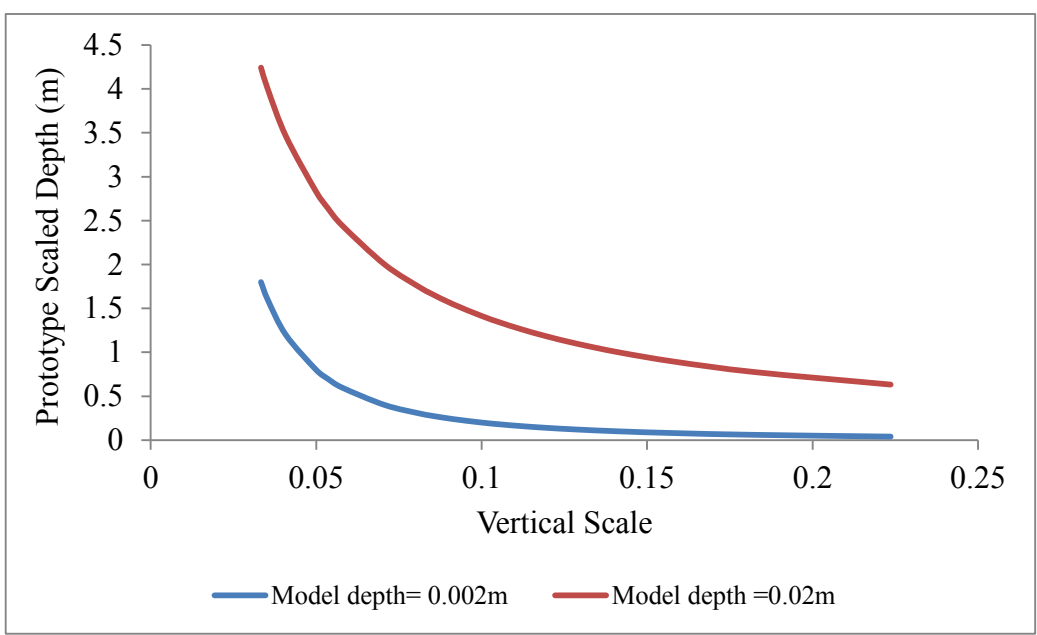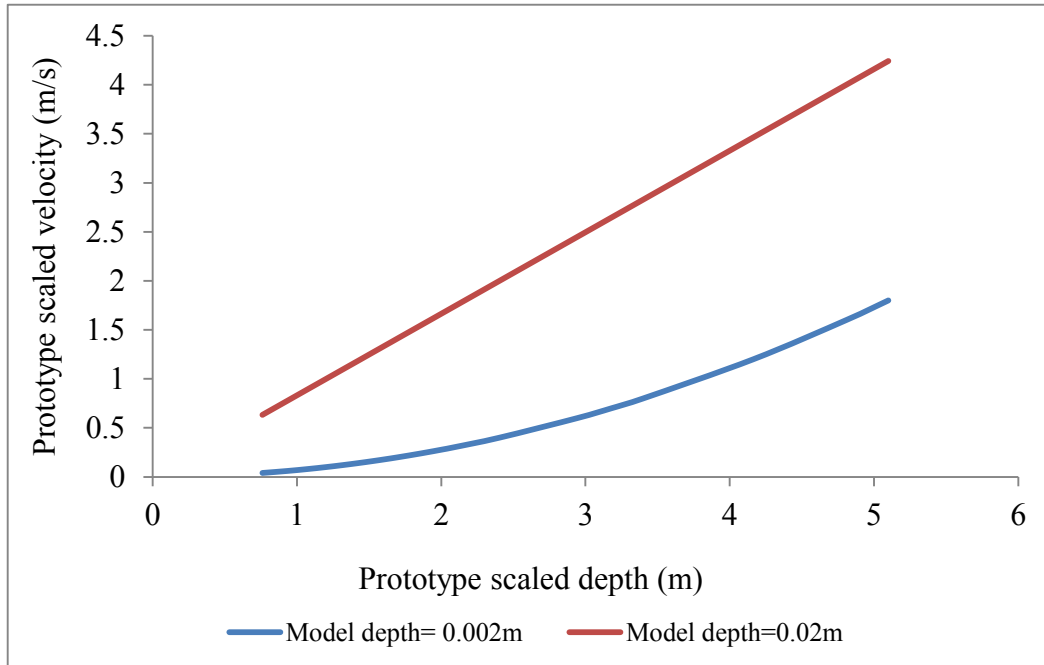

Figure 4.8: Depth of the Prototype as Affected by the Depth of the Model for Different Vertical Scales

Figure 4.9: Prototype Scaled Velocity versus Scaled Depth as Determined by the Depth of the Model

A summary of the model scaling is presented in Table 4.6. The movable bed model of the "virtual river" is a distorted physical model with 1:700 horizontal and 1:200 vertical scales. The distortion factor is therefore 3.5, in keeping with the assumption made in the methods section. Based on the length of the model, the scaled length of the created prototype was estimated to be 2800 m. The velocity scale is approximately 1:14 which corresponds to a scaled velocity of 2.4 m/s in the prototype when the model's velocity is 0.17 m/s. The discharge scale is 1:2 000 000; therefore, a discharge of 4.7×10^{-4} m^3/s in the model would be equivalent to a discharge of 931 m^3/s in the field. The hydraulic timescale determined by using Froude similarity criteria was found to be 1:50. The depth of model was roughly estimated to be 0.002 m; when scaled to the full scale, it represents 0.4 m (Table 4.5) which was deemed too shallow to illustrate the situation in the field. As a result, a depth 10 times larger than the measured depth in the model was chosen in order to obtain a higher value of the depth in the virtual prototype. Therefore, the depth of the

prototype was 2 m. The Froude number is equal to 1.21 in both the model and the virtual

prototype. Thus, the model and the created prototype are hydraulically similar. The slope of the

prototype was 3.5 times smaller than the slope of the model which is in agreement with Sharp's

(1981) assertion (i.e. in a distorted model the slope of the model will increase proportionally to

the distortion factor).

Table 4.6: Hydraulic Scaling Summary

Variable	Model values	Prototype values (scaled)	Horizontal scale	Vertical scale	Velocity scale	Discharge scale	Time scale
Length (m)	4	2800	1:700	1:200	1:14	1:2000000	1:50
Max Q (m³/s)	0.00047	931					
Velocity (m/s)	0.17	2.4					
Depth (m)	0.02	2					
Slope	0.04	0.011					
Froude number	1.21	1.21					

A summary of sediment scaling is detailed in Table 4.7. The particles of the created

prototype have a scaled median size of 7.1 mm. The grain Reynolds number (Re^*) scale is 1:40

which yields a scaled grain Reynolds number of 2379 in the prototype for a grain Reynolds

number of 58.88 in the model. As it can be noted in Table 4.7, the particle Reynolds number in

the model is different from the particle Reynolds number in the prototype. The Shields stress

scale (τ^*) is about 1:1.24 which corresponds to a scaled Shields stress value of 1.95 in the created

prototype for a corresponding value of 1.58 in the model. Those results suggest that the model

and the prototype are not fully similar. This seems reasonable, for complete similitude between a

model and its prototype is not easily achievable due to the difficulty of controlling all the factors

involved in the process. The hydraulic time scale was multiplied by a factor of 10 in order to find

the sediment time scale (1:4.95) according to Zwamborn (1966). Based on the sediment time

scale, 30 minutes in the prototype are equivalent to two and a half days in the prototype.

Table 4.7: Sediment Scaling Summary

Variable	Model values	Prototype values	Re^* scale	τ^* scale	Time scale
D_{50}(mm)	0.94	7.1	1:40	1:1.24	1:4.95
Re^*	58.88	2379			
τ^*	1.58	1.95			

CHAPTER 5

CONCLUSIONS AND RECOMMENDATIONS

5.1 Conclusions

The present research investigated the suitability of the coded-by-size thermoset plastic media used as sediment in the Emriver model by determining its basic properties (e.g. particles size distribution and specific gravity). Equally important was the application of the Engelund-Hansen and the Schoklitsch equations to establish the type (s) of bed channel epitomized by the media. Of interest was also the creation of a virtual river reach from hydraulic and sediment data available in the Emriver model. The experimental methods included mobile bed experiments and use of similitude and scaling theories.

Results show that thermoset plastic media satisfies the basic criteria to be used as model sediment in regard to the particles size and specific gravity. The Engelund-Hansen and the Schoklitsch equations made a fair prediction of sediment transport rates in the Emriver model, exclusively with increasing slope and Froude number. Using the predictions of Engelund-Hansen's and Schoklitsch's equations, the thermoset plastic media was classified as both coarse sand and gravel.

By applying similitude and scaling relations, it was possible to establish good hydraulic and sedimentary similitude between the model and the created prototype. However, in practice, some adjustments (e.g. slope, discharge) will have to be made in the model in order to achieve similarity.

5.2 Recommendations

Although the thermoset plastic media meets the basic criteria to be used in modeling, the particular processes that it can replicate remain unknown. Furthermore, due to the coarse size of its particles, the media was not shown to be suitable for suspended sediment transport. Additional investigations are also necessary to determine some other important properties for the media (e.g. the roughness coefficient; critical velocity for incipient motion). Finally, subsequent studies are needed in order to establish the conditions under which some features of a known prototype can be replicated in the model.

References

1. Allen, J. (1952). "Construction of river models; devices for measuring depths and velocities." *Scale models in hydraulic engineering*, Longmans, Green & Co., London.

2. Ashmore, P.E. (1991). "How do gravel-bed rivers braid?" *Canadian Journal of Earth Science* 28: 326-341.

3. Bettess, R. (1990). "Survey of lightweight sediments for use in mobile-bed physical models." Shen, H.W. (Ed.), *Movable bed physical models*, Kluwer Academic publishers, 115-123.

4. Bravo-Espinosa, M. Osterkamp, W.R., and Lopes, V.L. (2003). "Bed-load transport in alluvial channels". *Journal of Hydraulic Engineering*, ASCE 129 (10), 783-795.

5. Dalrymple, R. A. (1985). "Introduction to physical models in coastal engineering." *Physical modeling in coastal engineering*, Ed., A.A. Balkema, Rotterdam, The Netherlands.

6. Das, B.M. (2002). *Soil mechanics laboratory manual*, 6th Ed., Oxford University Press, Inc., New-York.

7. Ettema, R., Arndt, R., Roberts, P., and Walhl, T. (2000). *Hydraulic modeling concepts and practice,* 2000 manuals and reports on engineering practice no 97. ASCE, Reston, Virginia.

8. Fan, N.L., and Le Méhauté, B. (1969). *Coastal movable bed scale model technology*, Final report prepared for US Army, Coastal Engineering Center. Tetra Tech.

9. Foster, J. E. (1975). "Physical modeling techniques used in river models." *Symposium on Modeling Techniques*, ASCE, Reston, Va

10. Franco, J. J. (1978). "Guidelines for the design, adjustment and operation of models for the study of river sedimentation problems." *Instruction Rep. No. H-78-1*, U.S. Army Engineer Waterways Experiment Station, Vicksburg, Miss

11. Gaines, R. A. (2002). "Micro-scale movable bed physical model." Ph.D. thesis, Univ. of Missouri-Rolla, MO.

12. García, M. H. (2008). "Sediment transport and morphodynamics." *Sedimentation Engineering: processes, managements, modeling, and practice-ASCE Manuals and reports on Engineering Practice No 110.* ASCE, Reston, VA.

13. Glazik, G. (1984). "Influence of river model distortion on hydraulic similarity of structures arranged at the channel." *Symp. on Scale Effects in Modeling Hydraulic Structures*, Germany, International Association for Hydraulic Research, Esslingen, Germany.

14. Gough, S. (2011). Personal communication.

15. Ho, J., Coonrod, J., Gill, T., and Mefford, B. (2010). "Case study: Movable model scaling for bed-load sediment exclusion at intake structure on Rio Grande". *Journal of Hydraulic Engineering, ASCE*, 136 (4) 247-250.

16. Hughes, S. A. (1993). *Physical models and laboratory techniques in coastal engineering*, World Scientific Publishing Co. Pte. Ltd.

17. Jaeggi, M.N.R. (1986). "Non-distorted models for research on river morphology." *Symp. on Scale Effects in Modelling Sediment Transport Phenomena*, International Association for Hydraulic Research, Toronto.

18. Maynord, S. T. (2006). "Evaluation of the micromodel: an extremely small scale movable bed model". *Journal of Hydraulic Engineering*, 132 (4), 343-353.

19. Parker, G. (1998). "River meanders in a tray." *Nature,* Vol. 395, 111-112.

20. Peakall, J., Asworth, P., and Best, J. (1996). "Physical modeling in fluvial geomorphology: principles, applications and unresolved issues". Ed. by Rhoads, B.L. and Thorn, C.E., John Wiley &Sons Ldt. 221-253.

21. Raghunath, H.M. (1967). *Dimensional analysis and hydraulic model testing*, Asia Publishing House.

22. Rocha, J.S. (1990). "Movable bed models for gravel bed streams." Shen, H.W. (Ed.), *Movable bed physical models*, Kluwer Academic publishers, 81-90.

23. Sharp, J.J. (1981). "River models." *Hydraulic modeling*, Butterworth & Co. Ltd, London.

24. Thorne, C.R., Hey, R.D., and Newson, M.D. (1997). "Sediment erosion, transport and deposition." *Applied fluvial geomorphology for river engineering and management*, John Wiley & Sons, Chischester, New-York.

25. Van Rijn, L.C. (1993). *Principles of sediment transport in rivers, estuaries and coastal seas*, Aqua Publications, Netherlands.

26. Waldron, R. (2008). "Physical modeling of flow and sediment transport using distorted scaled modeling." Masters thesis, Louisiana State Univ., LA.

27. Warburton, J., and Davies, T. (1994). "Variability of bed-load transport and channel morphology in a braided river hydraulic model." *Earth Surface Processes and Landforms*, 19, 403-421.

28. Warnock, J.E. (1950). "Hydraulic similitude". *Engineering hydraulics*, Ed. by H. Rouse, John Wiley & Sons, New-York.

29. Whelan, T. (1994). *Polymer technology dictionary*, 1st Ed., Chapman & Hall, New
    Southgate London, UK.

30. Yalin, S.M. (1971). *Theory of hydraulic models*, The Macmillan Press Ldt, London and
    Basingstoke.

31. Yang, C. T., and Wan, S. (1991). "Comparisons of selected bed-material load formulas."
    Journal of Hydraulic Engineering, 117(8) 973-989.

32. Young, W. J. (1989). "Bed load transport in braided gravel-bed rivers: a hydraulic model
    study." Ph.D. thesis, Univ. Canterbury, NZ.

33. Young, W.J., and Davies, T.R.H. (1990). "Prediction of bed-load transport rates in
    braided rivers: a hydraulic model study." *Journal of Hydrology* (NZ), 29(2), 75-92.

34. Zwamborn, J.A. (1966). "Reproducibility in hydraulic models of prototype river
    morphology." *La Houille Blanche*, N$_o$3, 291-298.

VITA

Graduate School
Southern Illinois University

Jean-Rene Thelusmond

tjrene2004@yahoo.fr

State University of Haiti
Bachelor of Science, Natural Resources & Environment, September 2006

Southern Illinois University Carbondale
Master of Science in Civil and Environmental Engineering, August 2011

Thesis Title:
    The Use of Plastic Media in a Movable Bed Model to Study Sedimentary Processes in
Rivers

Major Professor: Dr. Lizette R. Chevalier